ICSI 2021 The 4th International Conference on Structural Integrity

# Effect of elliptical defect orientation on the durability of specimens subjected to cyclic bending

Zbigniew Marciniak[a]*, Ricardo Branco[b], Rui F. Martins[c], Dariusz Rozumek[a], Wojciech Macek[d]

[a]*Opole University of Technology, Department of Mechanics and Machine Design, ul. Mikolajczyka 5, 45-271 Opole, Poland*
[b]*CEMMPRE, Department of Mechanical Engineering, University of Coimbra, Rua Luís Reis Santos, Pinhal de Marrocos, 3030-788 Coimbra, Portugal*
[c]*UNIDEMI, Department of Mechanical and Industrial Engineering, Nova School of Science and Technology, Universidade NOVA de Lisboa, Campus de Caparica, 2829-516 Caparica, Portugal*
[d]*Gdańsk University of Technology, Faculty of Mechanical Engineering and Ship Technology, 11/12 Gabriela Narutowicza, Gdańsk, 80-233, Poland*

## Abstract

This work presents the effect of elliptical defects orientation on the durability of specimens made of C45 steel. Three kinds of specimens with elliptical defects in the form of a one-sided notch oriented at different angles 45, 60, and 90 degrees were subjected to cyclic bending (R=-1). The stress state analysis was performed using local and non-local methods to determine an equivalent amplitude of stress, and then the results were compared with those obtained for smooth specimens.

*Keywords:* Fatigue of material; Non-local methods; Defects.

## 1. Introduction

The awareness of defects existence, despite more and more perfect production processes, in the structure of the material, and thus also in the structure, stimulates the scientific world to check their impact on durability. In their

* Corresponding author. Tel.: +48 774498422.
E-mail address: z.marciniak@po.edu.pl

works, the researchers try to take into account various geometric parameters to best describe the influence of these features on the strength of the structural element.

Torib et al. performed tests on samples made of eutectoid steel (with a pearlitic structure). The prefabricates used for the samples were made in two different technological processes. In the first process, the bar was hot rolled, while the second was obtained in the cold drawing process. As a result of these two processes, the obtained sample surfaces differed from each other. Their strength properties were also different. Cold drawn bars are characterized by a much higher yield point and a higher tensile strength index. In both cases, micro defects were observed on the surface of the samples, but for cold drawn bars they were several times smaller. In both cases, the defects were the places of stress concentration and as a result, the cracks were initiated in these places. Hot-rolled steel samples, at a given load level, deteriorated faster than drawn samples. The authors unequivocally stated that the type of technological process is of great importance for the results of fatigue life tests.

Roy et al. (2012) analyzed high-cycle fatigue tests of samples made of A356-T6 aluminium alloy (ISO Al-Si7Mg) with natural surface imperfections and artificially introduced material losses. Pendulum cycle fatigue tests were carried out for three types of load, i.e. stretching, torsion and tension with torsion. The maximum size of defects for artificially introduced defects was 450 - 700 µm. Naturally occurring defects on the surface were in most cases in the range of 0 - 100 µm, and the maximum internal defects reached 300 - 500 µm. In the cyclic tensile test, it was noticed that artificial defects are undoubtedly the point of crack initiation, which was not so obvious for other types of defects in the sample material. Similar conclusions were drawn for the cyclic twisting test.

Gonzalez et al. (2014) analyzed the influence of casting defects and artificially introduced defects on the fatigue life of samples made of AS7G06 aluminium alloy (ISO AlSi7Mg0.6). The samples were subjected to the cyclic stretching test for two different cycle asymmetry coefficients R = - 1 and R = 0.1. In both cases, the analysis of the test results showed a clear decrease in the breaking stress with the increase in the size of the defect. The artificially introduced defects in the material had the size of 400 - 900 µm and then the maximum allowable stress level was much lower. Natural casting defects below 100 µm, in most cases, did not damage the sample within the tested range of the number of cycles. The authors noted that the fatigue strength drops significantly for defects with a size of 300 µm.

Mu et al. (2011) carried out tests of the fatigue life of the A319 aluminium alloy (ISO AlSi5Cu3) by subjecting it to cyclic tension-compression at room temperature and 130°C. It was shown that the increased temperature decreased the fatigue limit by 10%. In addition, analysis of the fractures of the samples showed that in all cases the damage originated in the pores near the outer surface of the sample. There was also a tendency to reduce the number of fatigue cycles with the increasing size of the defect in which the crack started.

Branco et al. (2021) presented the multiaxial fatigue behavior of 18Ni300 steel fabricated by selective laser melting. Hollow cylindrical specimens with transverse holes was subjected to bending-torsion fatigue. A one-parameter fatigue damage law showed good agreement in the fatigue lifetime estimation compared to the experimental.

Several authors have studied the impact of the size of the defect using various parameters to describe it. One of the most frequently used is the parameter proposed by Murakami (2002), i.e. the √area, which corresponds to the square root of the surface of the defect projected into the direction perpendicular to the load. Another method of analysis is the use of non-local fatigue calculation methods. These methods are currently very popular, as evidenced by the number of papers published in major scientific journals. In the group of these methods, there are four basic approach:

- point method (Taylor);
- the linear method in which the stresses are averaged in a straight line from the bottom of the notch into the specimen (Qylafku et al.);
- surface method, averaging stresses takes place on a specific surface (Seweryn, Susmel and Taylor);
- volumetric method, in which the volume is used to determine the non-local stress (Palin-Luc et al.).

The work aims to present the influence of elliptical defects on the fatigue life of samples subjected to bending.

**Nomenclature**

| | |
|---|---|
| $V_{cr}$ | critical volume |
| $f(\sigma_{ij})$ | stress function |
| $\sigma_y$ | yield strength |
| $\sigma_{UTS}$ | ultimate tensile strength |
| E | Young's modulus |
| $\sigma_x$ | stress in x-direction |
| $\sigma_1$ | first principal stress |
| $\sigma_{H-M}$ | stress calculated according to the Huber-Mises-Hencky hypothesis |

## 2. Material and tests

The experimental tests were performed on the MZGS-100Ph fatigue test stand (Kasprzyczak et al. (2013) and Rozumek and Marciniak (2012)), on which the samples were subjected to cyclic bending. The loads were selected so that the tests were carried out in the field of high-cycle fatigue.

Higher quality structural steel marked with the symbol C45, commonly used for medium-loaded and wear-resistant machine parts, was selected for fatigue tests. The chemical composition and mechanical properties are presented in Tables 1 and 2.

Fig. 1 shows the structure of the tested steel. The material was characterized by a ferritic-pearlitic structure, and the percentage of perlite was 52%. The grains of perlite and ferrite are evenly distributed in the structure. The grain size is not very diversified and the average grain size is 6.44 µm.
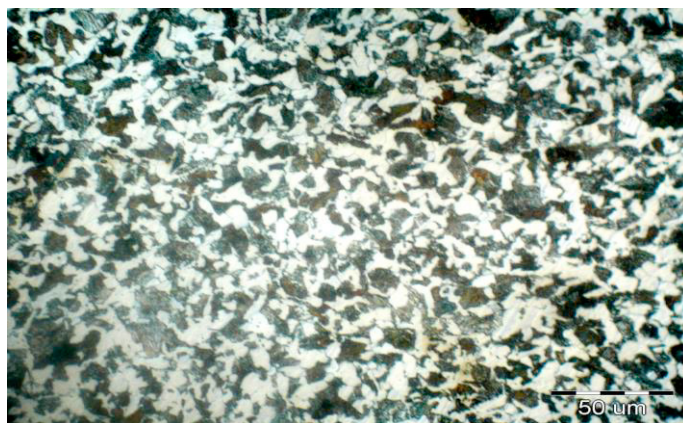


Fig. 1. Microstucture of C45 steel.

Table 1. Chemical composition of C45 steel.

| Element | C | Si | Mn | Cr | Ni | S | P | Cu | Fe |
|---|---|---|---|---|---|---|---|---|---|
| Content % | 0.42-0.5 | 0.17-0.37 | 0.5. 0.8 | max. 0.3 | max. 0.3 | max. 0.04 | max. 0.04 | max. 0.3 | Bal. |

Table 2. Mechanical properties.

| $\sigma_y$ | $\sigma_{UTS}$ | $\nu$ | E | $A_5$ |
|---|---|---|---|---|
| MPa | MPa | | GPa | % |
| 547 | 739 | 0.3 | 215 | 17 |

Four types of samples, of diameter 10 mm, were tested: smooth (without a defect), with a defect 3.5 mm long at an angle of 90°(Fig. 2a), with a defect of length 4 mm at an angle of 60° (Fig. 2b), with a defect of length 4.9 mm at an angle of 45° (Fig.2c). The defects were made employing wire electrical discharge machining (EDM) with a diameter of 0.64 mm to a depth of 0.32 mm. The defect system was designed in such a way that the Murakami parameter ($\sqrt{area}$) was the same for all defect samples.

The quality of the defects was checked on the Alicona Infinite G4 surface topography stand, where the area of the defect was scanned, and then, using the MountainsMap software, surface roughness and defect depth analyzes were carried out to eliminate samples with deviating geometric parameters (Macek et al.(2021)).
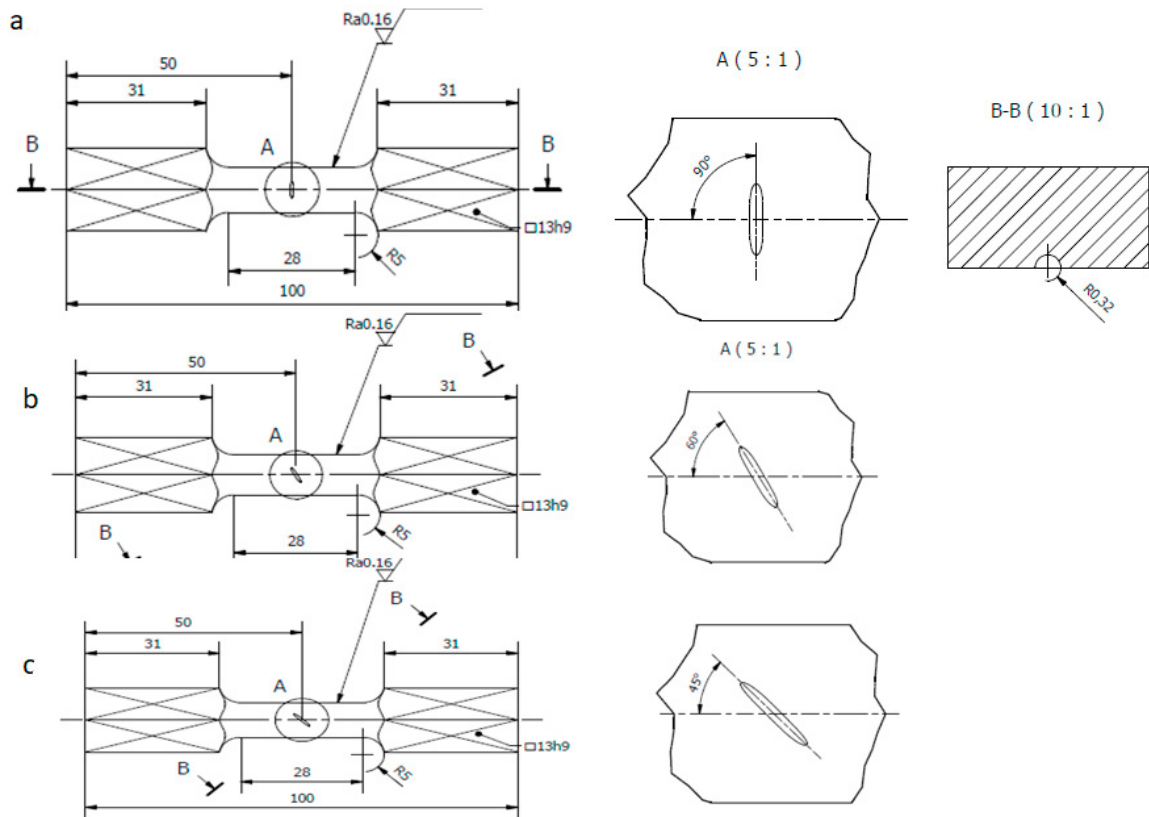


Fig. 2. Shape and dimension (in mm) of the tested specimens with the defect orientation angle (a) 90°, (b) 60°, (c) 45°.

## 3. Experimental results

The samples were loaded with various amplitudes of the bending moment, looking for the smallest amplitude value that would lead to the failure of individual types of samples. The damage was defined as a 20% decrease in the stiffness of the sample. The research was carried out in the field of high-cycle fatigue (HCF) with R = -1. The results of the fatigue tests are shown in Fig. 3. Based on the calculations made by the finite element method (FEM, Fig. 4), theoretical notch operation coefficients were determined, which are equal to 2.6, 2.34 and 2.04, respectively, for samples with a defect at the angle of 90, 60 and 45 degrees, and the determined stress values are shown in Fig. 5
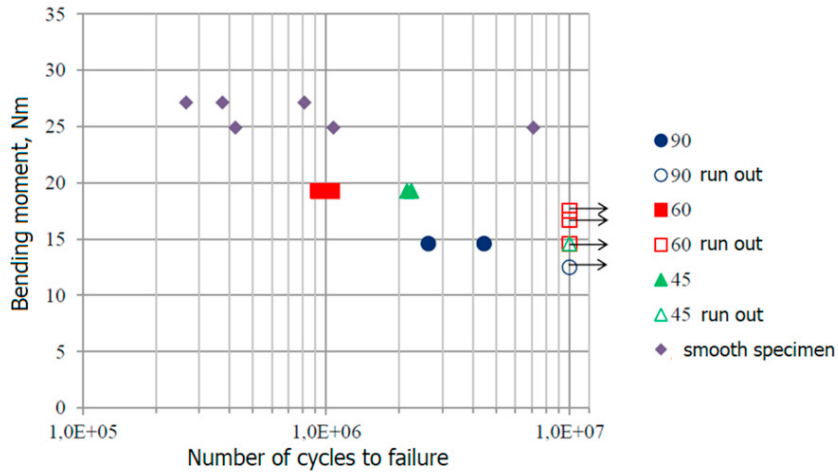
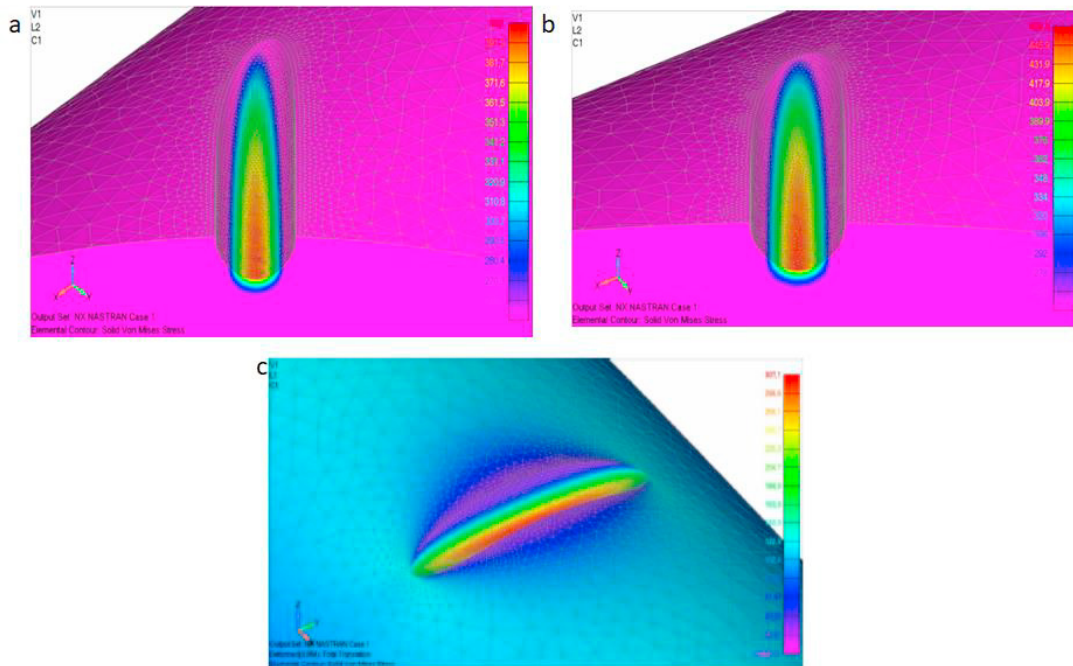Fig. 3. Diagram of the dependence of the number cycles to failure as a function of the bending moment.



Fig. 4. Stress distribution according to the Huber-Mises-Hencky hypothesis: (a) 45° and  (b) 60° for bending moment 19.3 N·m, (c) 90° for bending moment 11.6 N·m.
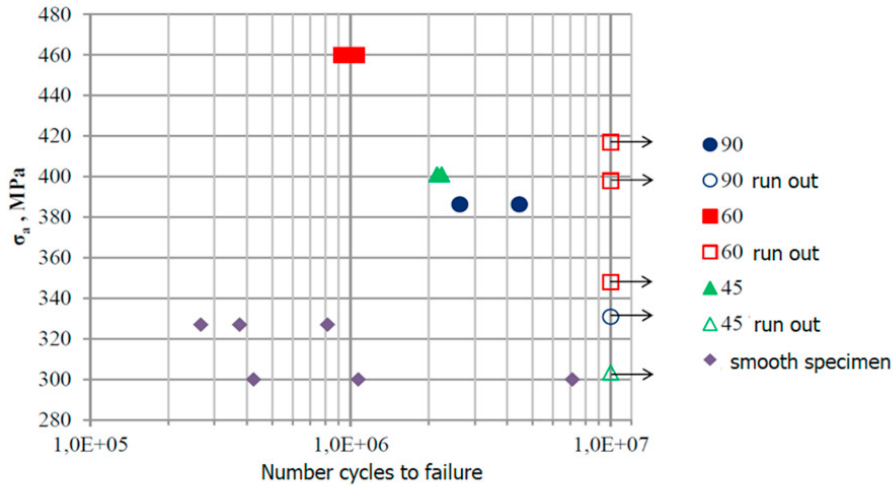
Fig. 5. S-N plot for stresses calculated using the theoretical notch factor.

The stress values determined by this method, and the S-N diagrams connected with it, indicate significant differences in values to smooth samples, despite similar durability, which may cause misinterpretations in design.

## 4. Non-local method approach

The next step in the analysis of the results of fatigue life was the application of the volumetric, non-local method(1) of fatigue calculations. For this purpose, the results of calculations using the finite element method were used, which enabled the determination of the volume in which the stress values are above the limit stress. This volume will be referred to as the critical stress volume later in the paper.

$$\sigma_{eq} = \frac{1}{V_{cr}} \int_{V_{cr}} f(\sigma_{ij}) dV \tag{1}$$

For the calculation of the equivalent stress, the stress of 300 MPa was selected as a reference level, which corresponds to the lowest value of the stress amplitude at which failure occurred in the tests of smooth samples. The determined volumes differed depending on the selected criterion (Table 3). As can be seen, the smallest volume of critical stresses is for the equivalent stress criterion according to the Huber-Mises hypothesis, and the largest for the principal stress.

Table 3. The size of the critical volume in mm$^3$.

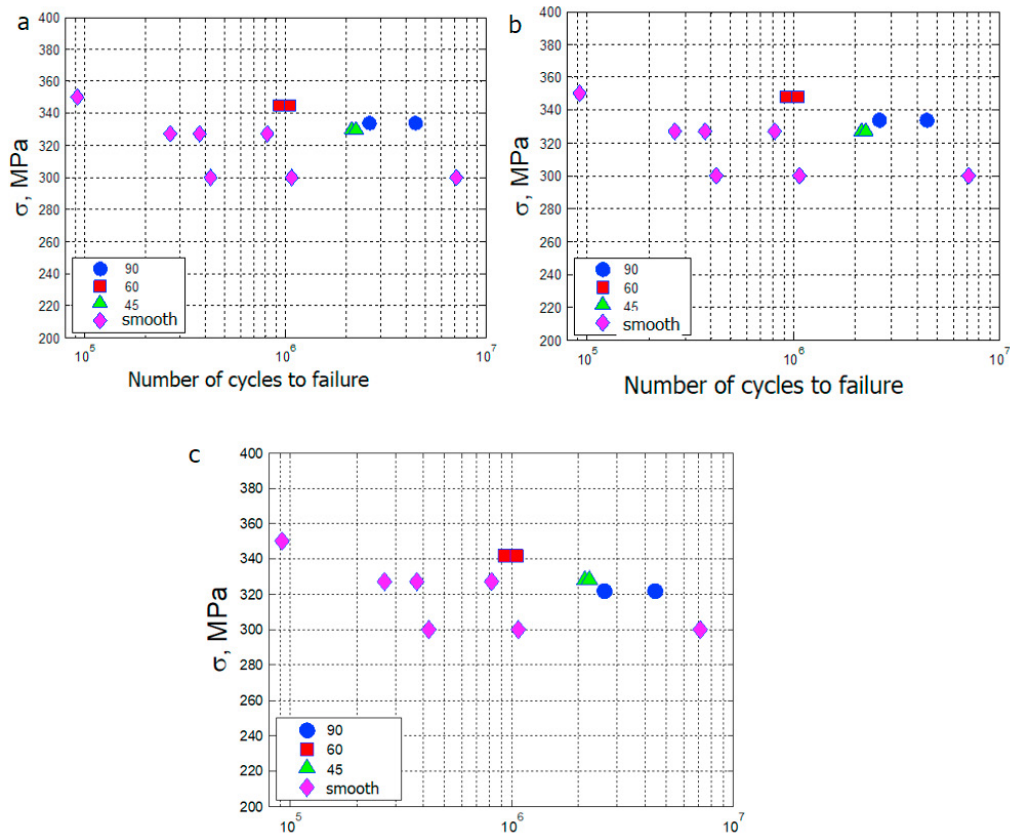|  | 45° | 45° | 45° |
|---|---|---|---|
|  | 19.3 Nm | 19.3 Nm | 14.6 Nm |
| $\sigma_{H-M}$ | 0.046 | 0.058 | 0.011 |
| $\sigma_x$ | 0.049 | 0.080 | 0.020 |
| $\sigma_1$ | 0.065 | 0.094 | 0.025 |

Fig. 6. S-N diagram for stresses calculated according to averaged: (a) normal stress $\sigma_{x\_ave}$ and (b) 1st principal stress $\sigma_{1\_ave}$, (c) Huber-Mises-Hencky hypothesis .

Analyzing the obtained results for the criteria selected above, a significant decrease in averaged stress concerning the stress values obtained from FEM calculations can be observed, and so for the sample with a defect at the angle of 60° the stress decreased by 120 MPa, for a sample with a defect at the angle of 45° by 70 MPa and a defect at the angle of 90° by 50 MPa. The results obtained by the non-local, volumetric method approximate the amplitude values of the samples with defects to the results of smooth samples.

Experiments also indicate that the defect configuration perpendicular to the longitudinal axis of the sample is the most harmful.

## 4. Summary

- The experimental tests show that the lowest bending moment value necessary to damage the sample occurs in the sample with the elliptical defect oriented perpendicular to the longitudinal axis of the sample.
- We learned from the results of fatigue testing that a specimen with a notch oriented at a 60-degree angle required a much higher stress level to fail than a specimen with a 45-degree notch despite the same bending moment values.
- The maximum sample stress does not always occur in the same sample geometry as the critical stress volumes
- Determination of equivalent stress using the non-local volumetric method showed that the values of these stresses came much closer to the stress values for smooth samples

**Future works:**
- Tests for torsional moments
- Tests for biaxial loads (bending and torsion) with in-phase and out-of-phase sequences

# References

Toribo. J, Matos J.-C., Gonzalez B., 2013 Role of Surface Defects in the Initiation of Fatigue Cracks in Pearlitic Steel. 13th International Conference on Fracture, Beijing, China

Roy M.J., Nadot Y., Nadot-Martin C., Bardin P.-G., Maijer D.M., 2011. Multiaxial Kitagawa analysis of A356-T6, International Journal of Fatigue; 33: 823-832

Gonzalez R., Martinez D. I., Gonzalez J. A., Talamantes J., Valtierra S., Colas R., 2014. Influence of casting defects on the fatigue behavior of cast aluminium AS7G06-T6, International Journal of Fatigue; 63: 97-109.

Mu P., Nadot Y., Nadot-Martin C., Chabod A., Serrano-Munoz I., Verdu C., 2011. Experimental investigation for fatigue strength of a cast aluminium alloy, International Journal of Fatigue; 33: 273-278

Branco R., Costa J.D., Martins Ferreira J.A., Capela C., Antunes F.V., Macek W., 2021. Multiaxial fatigue behaviour of maraging steel produced by selective laser melting, Mater. Des., 201 (2021), Article 109469, 10.1016/j.matdes.2021.109469

Murakami Y., 2002. Metal fatigue. Effects of Small Defects and Nonmetallic Inclusions. Elsevier, 369

Taylor D., 1999 Geometrical effects in fatigue: a unifying theoretical model, Int J Fatigue, 21, pp. 413-420

Taylor D.,2001. A mechanistic approach to critical-distance methods in notch fatigue, Fatigue Fract Engng Mater Struct, 24, pp. 215-24

Taylor D., 1998. The theory of critical distances, Engng Fract Mech, 75, 2008, pp. 1696-1705

Qylafku G., Azari Z., Kadi N., Gjonaj M., Pluvinage G. 1999. Application of a new model proposal for fatigue life prediction on notches and key-seats, Int J Fatigue, 21, pp. 753-760.

Qylafku G., Pluvinage G. 2001. Multiaxial fatigue criterion for notched specimens including the effective stress range, relative stress gradient, and hydrostatic pressure, Mater Sci, 37(4), pp. 573-582

Qilafku G., Kadi N., Dobranski J., Azari Z., Gjonaj M., Pluvinage G., 2001. Fatigue of specimens subjected to combined loading. Role of hydrostatic pressure, Int J Fatigue, 23, pp. 689-701

Seweryn A., Mróz Z., 1995. A non-local stress failure condition for structural elements under multiaxial loading, Engng Fract Mech 51(6), pp. 955-973

Susmel L., Taylor D., 2006. A simplified approach to apply the theory of critical distances to notched components under torsional fatigue loading, Int J Fatigue, 28, pp. 417-430

Palin-Luc T., Lasserre S.,1998. An energy based criterion for high cycle multiaxial fatigue, Eur J Mech., A/Solids, 17(2), pp. 237-251

Kasprzyczak L., Macha E., Marciniak Z., 2013. Energy parameter Control System of strength Machine for Material Test under cyclic bending and torsion, Mechatronic Systems and Materials IV 198, pp.489-494

Rozumek D., Marciniak Z., 2012. The investigation of crack growth in specimens with rectangular cross-sections under out-of-phase bending and torsional loading, Int. J. of Fatigue, Vol. 39, 81-87

Macek W., Marciniak Z., Branco R., Rozumek D., Królczyk GM., 2021. A fractographic study exploring the fracture surface topography of S355J2 steel after pseudo-random bending-torsion fatigue tests, Measurement, 178, 109443, 10.1016/j.measurement.2021.109443